Hindawi
Journal of Sensors
Volume 2017, Article ID 2596291, 11 pages
https://doi.org/10.1155/2017/2596291

Research Article

Water Level Sensing in a Steel Vessel Using A_0 and Quasi-Scholte Waves

Peng Guo,[1] Bo Deng,[1] Xiang Lan,[1] Kaili Zhang,[1] Hongyuan Li,[1] Zhenhua Tian,[2] and Hong Xu[1]

[1]*Key Laboratory of Condition Monitoring and Control for Power Plant Equipment of Ministry of Education, School of Energy, Power and Mechanical Engineering, North China Electric Power University, Beijing 102206, China*
[2]*Department of Mechanical Engineering and Material Science, Duke University, Durham, NC 27708, USA*

Correspondence should be addressed to Zhenhua Tian; zhenhua.tian@duke.edu

Received 15 July 2017; Accepted 25 October 2017; Published 20 December 2017

Academic Editor: Amardeep Kaur

Copyright © 2017 Peng Guo et al. This is an open access article distributed under the Creative Commons Attribution License, which permits unrestricted use, distribution, and reproduction in any medium, provided the original work is properly cited.

This paper presents a water level sensing method using guided waves of A_0 and quasi-Scholte modes. Theoretical, numerical, and experimental studies are performed to investigate the properties of both the A_0 and quasi-Scholte modes. The comparative study of dispersion curves reveals that the plate with one side in water supports a quasi-Scholte mode besides Lamb modes. In addition, group velocities of A_0 and quasi-Scholte modes are different. It is also found that the low-frequency A_0 mode propagating in a free plate can convert to the quasi-Scholte mode when the plate has one side in water. Based on the velocity difference and mode conversion, a water level sensing method is developed. For the proof of concept, a laboratory experiment using a pitch-catch configuration with two piezoelectric transducers is designed for sensing water level in a steel vessel. The experimental results show that the travelling time between the two transducers linearly increases with the increase of water level and agree well with the theoretical predictions.

1. Introduction

In power plants, monitoring the water levels in core facilities, such as the boiler steam drum, condensers, and cooling pipes, is critical for the safety and economical operation of power plants. Hence, there is a need to develop nondestructive technologies for high-precision, high-reliability, real-time monitoring of water levels in steel vessels. Ultrasonic guided waves have opened new opportunities for cost-effective nondestructive evaluation (NDE), because they can reveal small features related to the interaction between guided waves and structures and provide considerable information about the structures [1–4]. When a solid waveguide is immersed in water, the traction-free boundary condition changes and the wave propagation in the solid will change accordingly. When a free plate is immersed in water, the out-of-plane displacement in the plate can transmit into the water through the plate-water interface [1]. Worlton [5] extended the Lamb theory by using experimental observations and derived the dispersion curves for aluminum and zirconium plates. Bingham et al. [6] used ultrasonic guided waves to identify the mass loading on ship hulls. Na and Kundu [7] detected gouges and dents in an underwater pipeline using guided waves. Chen et al. [8] developed a damage identification approach using the A_0 mode for evaluating corrosion damage in submerged structures. Koduru and Rose [9] utilized an array of permanently mounted transducers to detect defects and avoid the influences from external environmental conditions, for example, water loading and temperature change. Pistone et al. [10] performed experimental studies using a pulsed laser for structural health monitoring of immersed aluminum plates. Yapura and Kinra [11] derived dispersion equations for a fluid-solid bilayer and then presented a numerical result for a water-aluminum bilayer. Baron and Naili [12] studied the fluid-loaded anisotropic and homogeneous plane waveguide with two different fluids on each side using an analytical approach. Yu and Tian [13] used a scanning laser Doppler vibrometer for measuring quasi-

Scholte waves in one-side water-immersed plates. Banerjee and Kundu [14] developed the distributed point source method (DPSM) to simulate the ultrasonic wavefields at the fluid and solid interface; their method can also be used to calculate the pressure, velocity, and displacement fields in the fluid.

For power plants, the frequently used water level measurement methods include the differential pressure gauge [15], ultrasonic level meter [16, 17], and radar level gauge [18]. For the differential pressure gauge, the water level is determined from the static pressure change induced by the water level change. Usually, there is a delay for determining the water level after the water level changes. In addition, the pressure condition might change due to the changes of temperature and other operation conditions. These factors could cause large errors in water level sensing. The ultrasonic level meter uses ultrasonic pulses reflected from the liquid-gas interface to determine the water level. In this method, ultrasonic pulses are generated by a transducer placed on the bottom of the container. Based on the travelling time of reflection waves, the water level is determined. However, large errors can be induced by poor reflection from the water surface and complex scattering waves in the container. The principle of radar level gauge is similar to the ultrasonic level meter, while the radar level gauge uses microwave pulses. In this method, the sensors need to be installed in the container, and thus the sensor installation may influence the integrity of the container and cause leakage. In addition, the water vapor on the waveguide tube might influence the signal quality.

In this paper, we present a water level sensing method for steel vessels by using guided waves of A_0 and quasi-Scholte modes. For water level sensing, two piezoelectric transducers (PZTs) are bonded on the out surface of the vessel in the pitch-catch configuration to generate and measure guided waves. The generated guided waves propagate in the wall of the vessel. The mode conversion between A_0 and quasi-Scholte modes at the water interface is observed. Based on the velocity difference between A_0 and quasi-Scholte modes, a quantitative method for detecting the water level is developed. Through proof-of-concept experiments, it has been found that the travelling time of guided waves in the vessel linearly increases with the increase of water level. Moreover, the experimental results agree well with theoretical predictions. The developed method provides several advantages. The method has a small error less than 3.7 mm, and sensors can be easily installed on the outer surface of the container without influencing the structural integrity. In addition, since the sensors are not in the container, the sensors can be easily maintained. Moreover, compared to the ultrasonic level meter, our method does not rely on the poor reflection from the water boundary and is less influenced by the scattering waves inside the container.

The rest of this paper is organized as follows. Section 2 presents the guided wave fundamentals, such as characteristic equations and dispersion curves for the free plate and the plate with one side in water. Section 3 presents the verifications of A_0 mode in the free plate and quasi-Scholte mode in the plate with one side in water through finite element simulations and experiments. Section 4 presents the water level sensing method with a proof-of-concept experiment. Section 5 concludes the paper with findings and future work.

2. Theoretical Fundamentals

2.1. Free Plates. Considerable research exists on the dispersion characteristics of guided waves in free isotropic plates [1, 2, 13, 19]. In this section, the dispersion characteristics of guided waves in a free plate with traction-free boundary conditions are given. For a free plate (in Figure 1(a)), the boundary conditions for the top and bottom surfaces of the plate can be described as follows:

$$\begin{aligned} \sigma_{xx}^{\mathrm{p\_t}} &= 0, \\ \sigma_{xz}^{\mathrm{p\_t}} &= 0, \\ \sigma_{xx}^{\mathrm{p\_b}} &= 0, \\ \sigma_{xz}^{\mathrm{p\_b}} &= 0, \end{aligned} \tag{1}$$

where $\sigma_{xx}^{\mathrm{p\_t}}$ and $\sigma_{xz}^{\mathrm{p\_t}}$ are the normal and shear stresses on the top surface of the plate, respectively. $\sigma_{xx}^{\mathrm{p\_b}}$ and $\sigma_{xz}^{\mathrm{p\_b}}$ are the normal and shear stresses on the bottom surface of the plate, respectively. The characteristic equation of Lamb waves in a free plate can be expressed as follows:

$$\begin{vmatrix} k_{sx}^2 - k_z^2 & k_{sx}^2 - k_z^2 & -2k_{sx}k_z & 2k_{sx}k_z \\ 2k_{lx}k_z & -2k_{lx}k_z & k_{sx}^2 - k_z^2 & k_{sx}^2 - k_z^2 \\ \left(k_{sx}^2 - k_z^2\right)e^{ik_{lx}d} & \left(k_{sx}^2 - k_z^2\right)e^{-ik_{lx}d} & -2k_{sx}k_z e^{ik_{sx}d} & 2k_{sx}k_z e^{-ik_{sx}d} \\ 2k_{lx}k_z e^{ik_{lx}d} & -2k_{lx}k_z e^{-ik_{lx}d} & \left(k_{sx}^2 - k_z^2\right)e^{ik_{sx}d} & \left(k_{sx}^2 - k_z^2\right)e^{-ik_{sx}d} \end{vmatrix} = 0, \tag{2}$$

where $k_{lx}^2 = \omega^2/c_{\mathrm{L}}^2 - k_z^2$, $k_{sx}^2 = \omega^2/c_{\mathrm{S}}^2 - k_z^2$, $k_z = 2\pi/\lambda_{\mathrm{wave}}$, $c_{\mathrm{L}} = \sqrt{[2\mu(1-\nu)]/[\rho(1-2\nu)]}$, and $c_{\mathrm{S}} = \sqrt{\mu/\rho}$. k_z is the wavenumber of Lamb waves. d is the plate thickness. ω and λ_{wave} are the circular frequency and wavelength, respectively. c_{L} and c_{S} are the velocities of longitudinal and shear waves, respectively. ρ, μ, and ν are the density, shear modulus, and

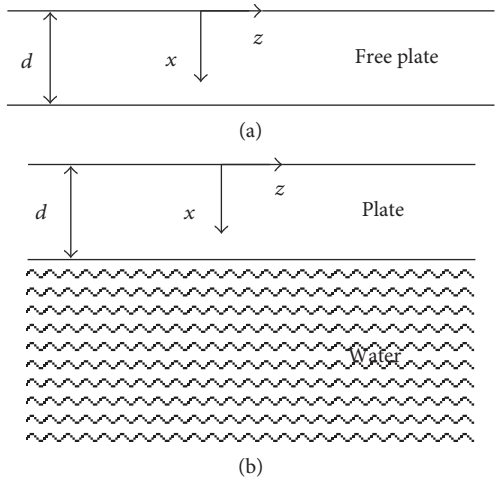

Figure 1: Sketches of (a) a free plate and (b) a plate with one side in water.

Poisson's ratio of the plate, respectively. By solving (2), the dispersion curves for a steel plate (the material properties of the steel plate are listed in Table 1) are obtained, as shown in Figures 2(a) and 2(b). In the low-frequency region, the group velocity of S_0 mode is relatively high. In contrast, the group velocity of A_0 mode is relatively low and changes greatly with respect to frequency.

Table 1: Material properties for a steel plate and water.

Stainless steel plate	Density (kg/m^3)	8000
	Young's modulus (GPa)	196.5
	Poisson's ratio	0.29
	Thickness (mm)	1.2
Water	Density (kg/m^3)	1000
	Bulk wave velocity (m/s)	1500

2.2. Plates with One Side in Water. As shown in Figure 1(b), when the bottom surface of a free plate is in water, its boundary conditions change compared to a free plate. Under the nonviscosity assumption, the boundary conditions for the bottom surface become

$$\begin{aligned} \sigma_{xx}^{\text{p\_b}} &= \sigma_{xx}^{\text{water}}, \\ \sigma_{xz}^{\text{p\_b}} &= 0, \\ u_{xx}^{\text{p\_b}} &= u_{xx}^{\text{water}}, \end{aligned} \tag{3}$$

where $u_{xx}^{\text{p\_b}}$ is the normal displacement on the bottom surface of the plate. u_{xx}^{water} and $\sigma_{xx}^{\text{water}}$ are the normal displacement and stress at the plate-water interface, respectively. The characteristic equation for the plate with one side in water can be assembled and expressed as follows:

$$\begin{bmatrix} k_{sx}^2 - k_z^{\,2} & k_{sx}^2 - k_z^{\,2} & -2k_{sx}k_z & 2k_{sx}k_z & 0 \\ 2k_{lx}k_z & -2k_{lx}k_z & k_{sx}^2 - k_z^{\,2} & k_{sx}^2 - k_z^{\,2} & 0 \\ \left(k_{sx}^2 - k_z^{\,2}\right)e^{ik_{lx}d} & \left(k_{sx}^2 - k_z^{\,2}\right)e^{-ik_{lx}d} & -2k_{sx}k_z e^{ik_{sx}d} & 2k_{sx}k_z e^{-ik_{sx}d} & \dfrac{\omega^2\rho_{\text{w}}}{\mu} \\ 2k_{lx}k_z e^{ik_{lx}d} & -2k_{lx}k_z e^{-ik_{lx}d} & \left(k_{sx}^2 - k_z^{\,2}\right)e^{ik_{sx}d} & \left(k_{sx}^2 - k_z^{\,2}\right)e^{-ik_{sx}d} & 0 \\ k_{lx}e^{ik_{lx}d} & -k_{lx}e^{-ik_{lx}d} & -k_z e^{ik_{sx}d} & -k_z e^{-ik_{sx}d} & \gamma \end{bmatrix} = 0, \tag{4}$$

where $\gamma^2 = \omega^2/c_{\text{Lw}}^2 - k_z^2$ and $c_{\text{Lw}} = \sqrt{\lambda_{\text{w}}/\rho_{\text{w}}}$. c_{Lw} is the bulk velocity in water; λ_{w} and ρ_{w} are the bulk stiffness and density of water, respectively. By solving (4), the dispersion curves of a 1.2 mm thick steel plate with one side in water are obtained. As shown in Figures 2(c) and 2(d), the fundamental antisymmetric and symmetric modes are denoted as $A_{0\text{w}}$ and $S_{0\text{w}}$. Compared to dispersion curves for a free plate (Figure 2(a)), dispersion curves for a plate with one side in water (Figure 2(c)) clearly show another mode, the quasi-Scholte mode, in addition to the fundamental antisymmetric and symmetric modes. The dispersive behavior of the quasi-Scholte mode in the plate with one side in water is the same as the mode discovered in a two-side water-immersed plate in [20]. The quasi-Scholte mode is dispersive in the low-frequency region; however, with the increase of the frequency, the mode gradually approaches the nondispersive Scholte mode (interface wave at solid and liquid interface) [20, 21].

3. Simulation and Experimental Studies

In the previous section, the dispersion curves of guided waves in a free plate and a plate with one side in water are theoretically studied. In this section, the quasi-Scholte and A_0 modes are further investigated through finite element simulations and experiments.

3.1. Verification of the A_0 Mode in a Free Plate. Finite element simulations are performed using the commercial software ANSYS to analyze the propagation of A_0 mode in a free plate. The finite element model of a plate's cross section is built using 2D elements (8-node PLANE82). Table 1 gives the

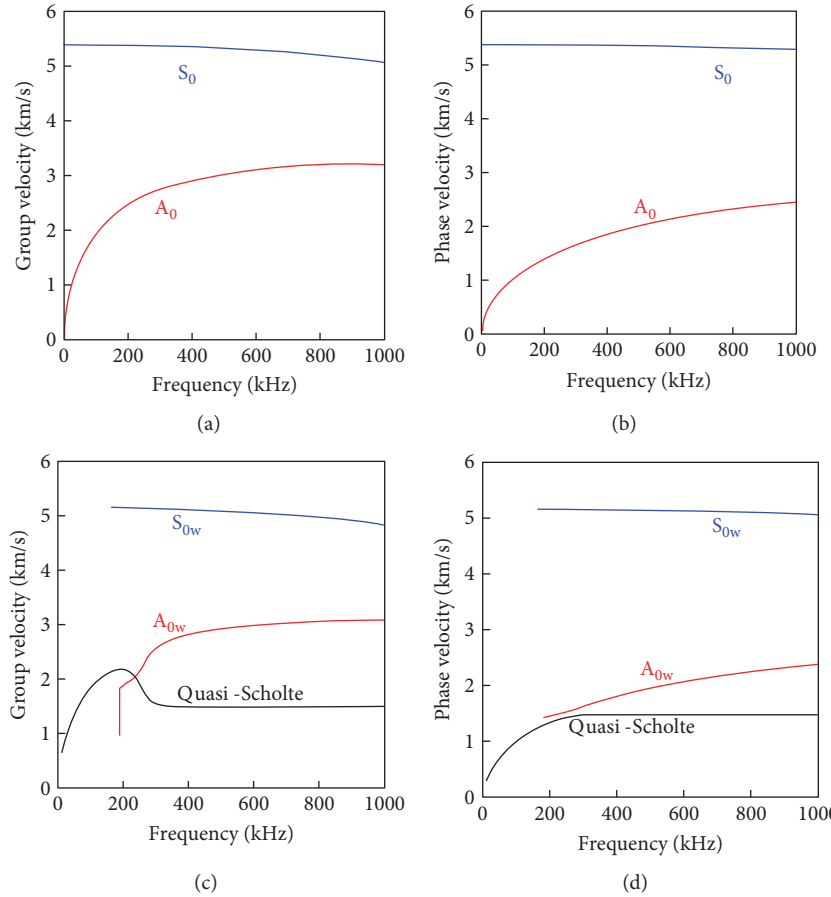

Figure 2: Theoretical dispersion curves: (a) and (b) are group and phase velocities for a 1.2 mm thick steel plate; (c) and (d) are group and phase velocities for a 1.2 mm thick steel plate with one side in water.

material parameters of the plate. The thickness and length of the plate are 1.2 mm and 100 mm, respectively. For simulating elastic waves in solids using finite element method (FEM), the transient analysis in ANSYS is adopted. To ensure the accuracy of the simulation, the grid size and the integral time step satisfy the following:

$$L_{\max} < \frac{\lambda_{\min}}{n_{\min}} = \frac{c_{\min}}{n_{\min} f}, \qquad \Delta t \le \frac{L_{\min}}{c_s}, \tag{5}$$

where $L_{\max}$ and $L_{\min}$ are the maximum and minimum grid size, respectively; $\lambda_{\min}$ is the minimum wavelength; $n_{\min}$ is the minimum number of elements within one wavelength (usually $n_{\min}$ is in the range of 8~10); c_s denotes the velocity of shear waves; and $c_{\min}$ is the minimum group velocity of elastic waves. Vertical loads are applied on the nodes at $X = 0$ on top and bottom surfaces, for generating a pure A_0 mode.

Figure 3 shows the simulation result (a vector field of displacement) for the A_0 mode, when the excitation is 5-count tone bursts at 100 kHz. From the result, it can be seen that the A_0 mode is antisymmetric. In addition, the vertical displacement is much stronger than the horizontal displacement. The displacement signals at four different locations ($X = 20$, 40, 60, and 80 mm on the bottom surface of the plate) are plotted in Figure 4. Using the traveling time and propagation distance, we can calculate the group velocity of A_0 mode, 1.92 mm/μs, which agrees well with the theoretical velocity 1.925 mm/μs.

An experiment is performed using the setup in Figure 5(a), for wave mode verification. Two PZT transducers (with dimensions of $7 \times 7 \times 0.2$ mm) in a pitch-catch configuration are adopted. The distance between two transducers is 150 mm. The excitation signal is 2.5-cycle tone bursts at 100 kHz. Figure 6 plots a received signal with its Hilbert envelope. Using the travelling time obtained from the received signal and the distance between two transducers, the group velocity of A_0 mode is calculated, which is 1.89 mm/μs. Figure 7 compares the A_0 mode's group velocities obtained from the theory, simulation, and experiment at 50, 100, and 150 kHz. The results of the theory, simulation, and experiment agree well with each other.

3.2. Verification of the Quasi-Scholte Mode in a Plate with One Side in Water. Finite element simulations are performed to analyze the propagation of quasi-Scholte mode in a plate with one side in water. Figure 8(a) plots a schematic of the

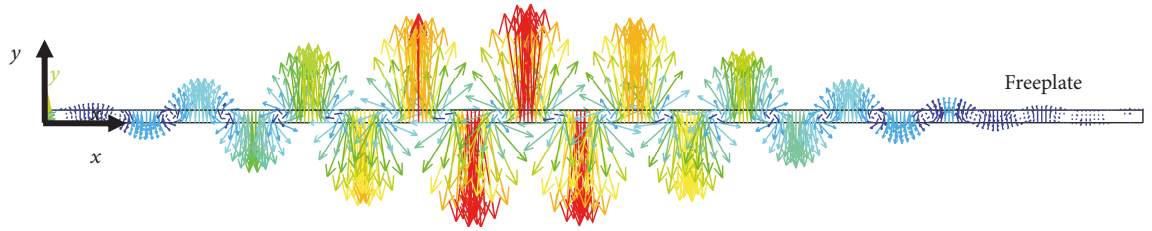

FIGURE 3: The FEM simulation result (displacement vector field) of the excited A_0 mode in a free plate at 100 kHz.

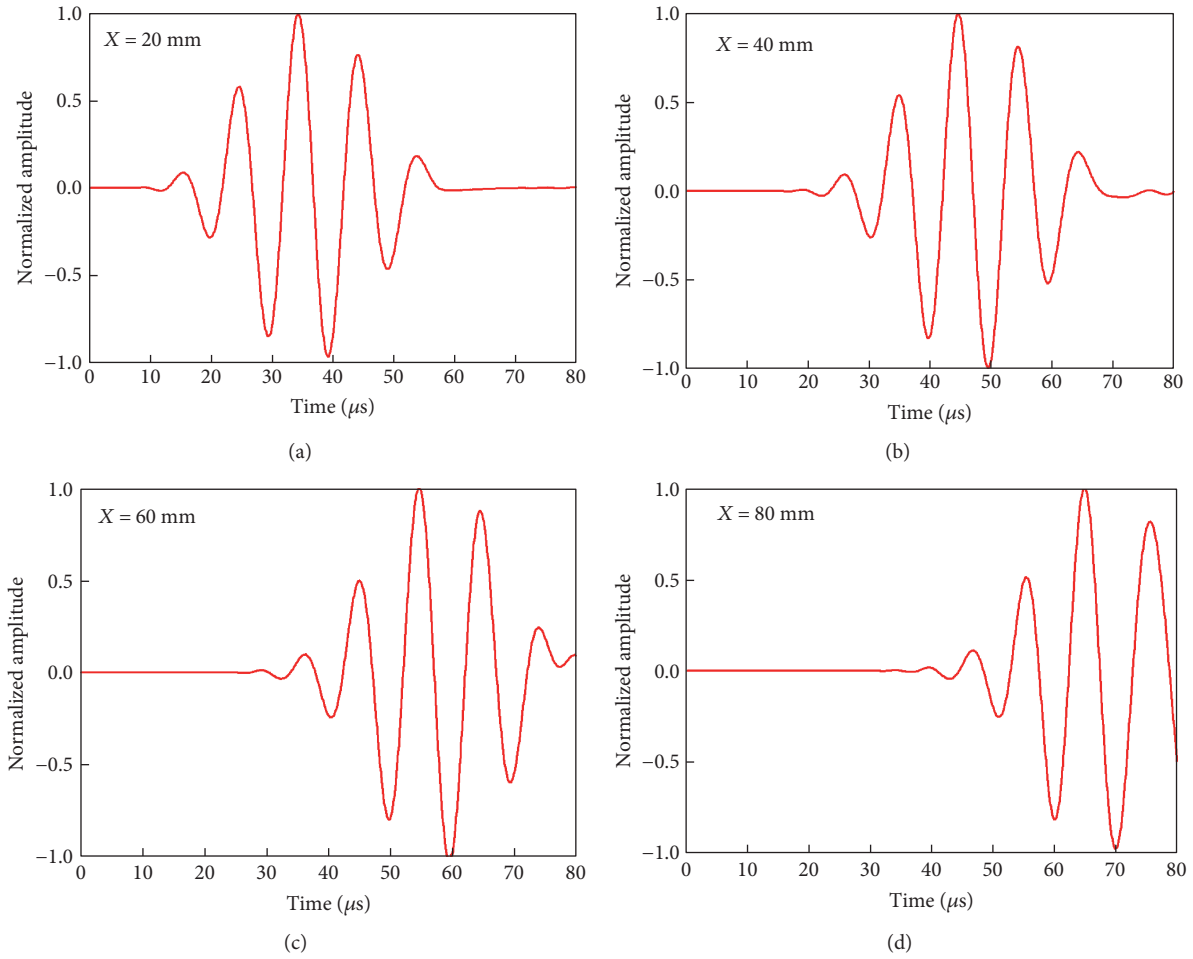

FIGURE 4: Out-of-plate displacement signals (simulation results) at different locations in the free plate. (a), (b), (c), and (d) are for $X = 20$, 40, 60, and 80 mm, respectively, on the bottom surface of the plate.

simulation setup. The top layer is a 1.2 mm thick steel plate. The bottom layer is water with the depth of 40 mm. In the finite element model, the water layer is created using the coupling field element (FLUID29).

Figure 8(b) shows the simulation result (pressure field) when the excitation is 5-count tone bursts at 100 kHz. In the water layer, it can be seen that there are two types of waves, the quasi-Scholte waves and pressure waves (P waves). The quasi-Scholte mode propagates along the interface between the plate and the water, while the P waves only propagate in water. The displacement signals at four different locations ($X = 20$, 40, 60, and 80 mm on the bottom surface of the plate) are plotted in Figure 9. Using the traveling time and propagation distance, we find the group velocity of the quasi-Scholte mode, 1.86 mm/μs at 100 kHz, which agrees well with the theoretical velocity 1.84 mm/μs.

An experiment is also performed using the setup in Figure 5(b), for wave mode verification. Two PZT transducers (with dimensions of $7 \times 7 \times 0.2$ mm) in a pitch-catch configuration are adopted. The distance between the two transducers is 150 mm. The excitation signal is 2.5-cycle tone bursts 100 kHz. Figure 10 plots a received signal with its Hilbert envelope, when the excitation frequency is 100 kHz. Using the received signal and the distance between two

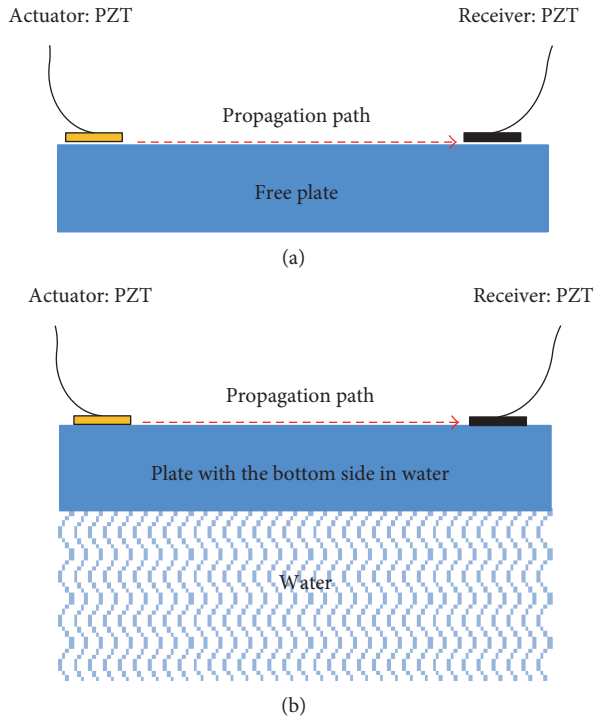

Figure 5: The experimental setup for guided wave sensing and mode identification: (a) in a free plate; (b) in a plate with one side in water.

transducers, the group velocity of A_0 mode is obtained, which is 1.85 mm/μs. Figure 11 compares the quasi-Scholte mode's group velocities obtained from the theory, simulation, and experiment at 50, 100, and 150 kHz. The results of theory, simulation, and experiment agree well with each other.

4. Water Level Sensing Using A_0 and Quasi-Scholte Modes

This section presents a water level sensing method by using both A_0 and quasi-Scholte modes. A pitch-catch sensing configuration with two PZT transducers is employed. For this configuration, a theoretical prediction of the relation between water level and wave travelling time is derived. For the proof of concept, a laboratory experiment is performed. The experimental results agree well with the theoretical predictions and show that the travelling time linearly increases with the increase of water level.

4.1. Theoretical Predictions. Figure 12 plots a proposed pitch-catch configuration with two PZT transducers for water level sensing. The full wave propagation path ($d_{\text{T-R}}$) consists of two parts: the water path d_{W} and the dry path $d_{\text{T-R}} - d_{\text{W}}$. In the water path d_{W}, the quasi-Scholte mode propagates in the plate with one side in water; in the dry path $d_{\text{T-R}} - d_{\text{W}}$, the A_0 mode propagates in the free plate. When the water level changes, it will directly change the portions of dry path $d_{\text{T-R}} - d_{\text{W}}$ and water path d_{W}. The guided waves leave the excitation PZT as the quasi-Scholte mode in the water path d_{W} and then are converted to the A_0 mode in the dry

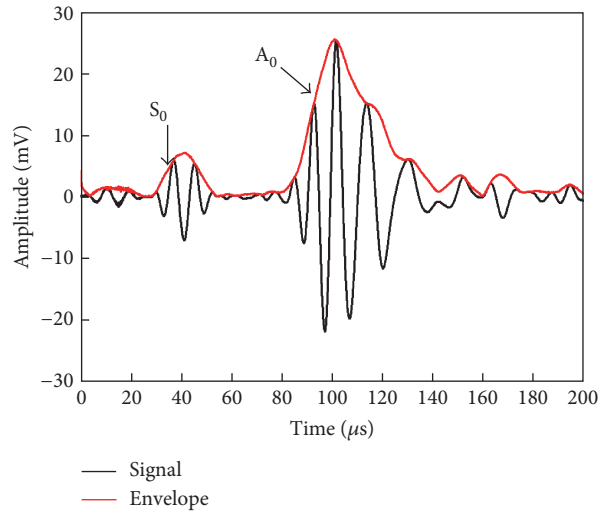

Figure 6: Experimental signal of guided waves in a free steel plate at 100 kHz.

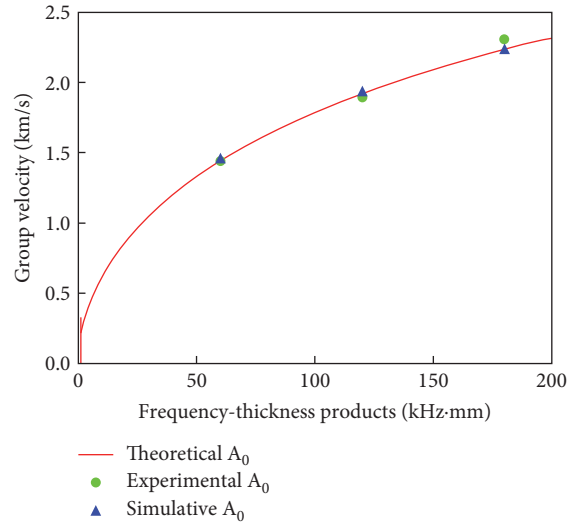

Figure 7: Comparison of A_0 mode's group velocities obtained from theory, simulation, and experiment.

path $d_{\text{T-R}} - d_{\text{W}}$. Therefore, the propagation time over the entire path $d_{\text{T-R}}$ is given by the following:

$$t_{\text{T-R}} = \frac{d_{\text{W}}}{c_{\text{QS}}} + \frac{d_{\text{T-R}} - d_{\text{W}}}{c_{A_0}}, \tag{6}$$

where c_{QS} is the quasi-Scholte mode group velocity, c_{A_0} is the A_0 mode group velocity, and $t_{\text{T-R}}$ is the propagation time over the entire propagation path $d_{\text{T-R}}$. If $d_{\text{W}} = 0$ is the baseline, when the water level d_{W} changes, the relation between time difference $\Delta t_{\text{T-R}}$ on the entire propagation path $d_{\text{T-R}}$ is given by the following expression:

$$\Delta t_{\text{T-R}} = d_{\text{W}} \left(\frac{1}{c_{\text{QS}}} - \frac{1}{c_{A_0}} \right). \tag{7}$$

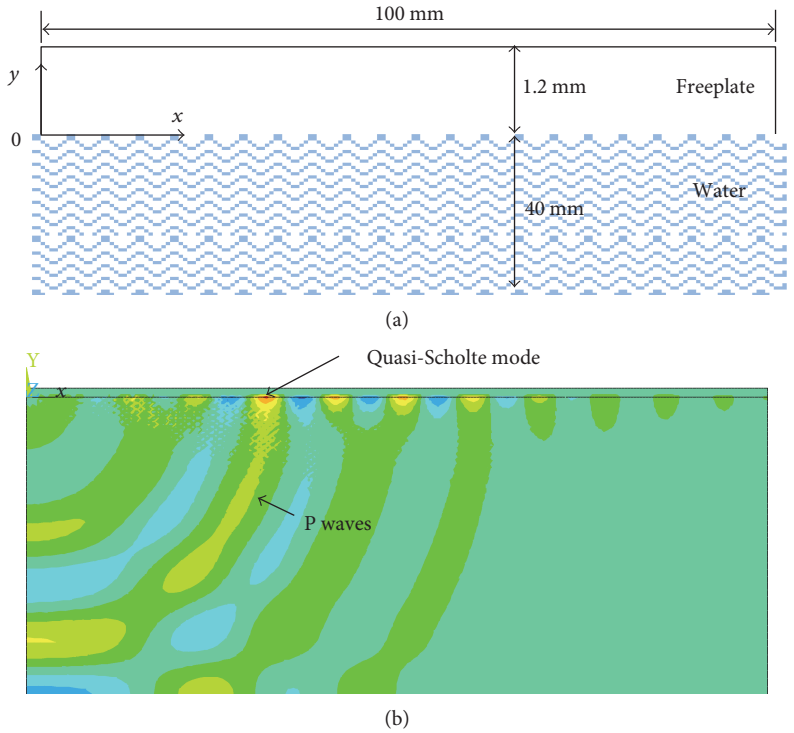

FIGURE 8: FEM simulation of the quasi-Scholte mode in a plate with one side in water at 100 kHz: (a) a schematic of the FEM model and (b) the simulation result (pressure field).

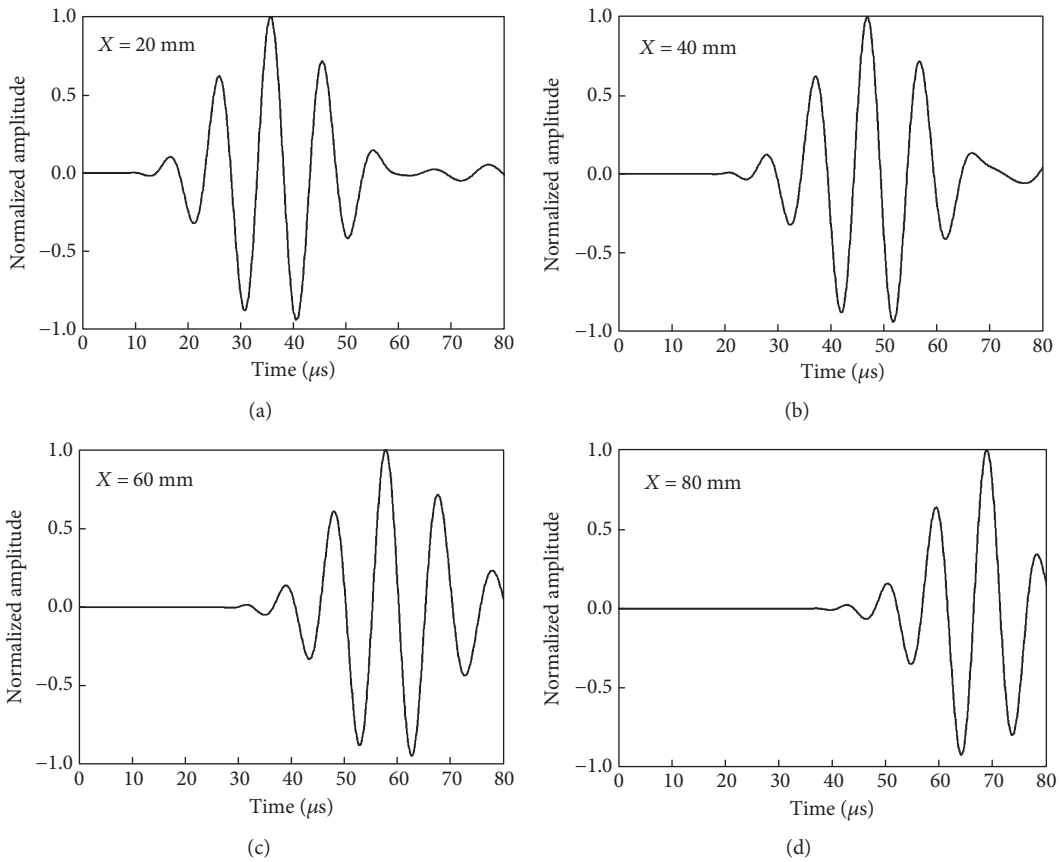

FIGURE 9: Out-of-plate displacement signals (simulation results) at different locations in the plate with one side in water: (a), (b), (c), and (d) are for $X = 20$, 40, 60, and 80 mm, respectively, on the bottom surface of the plate.

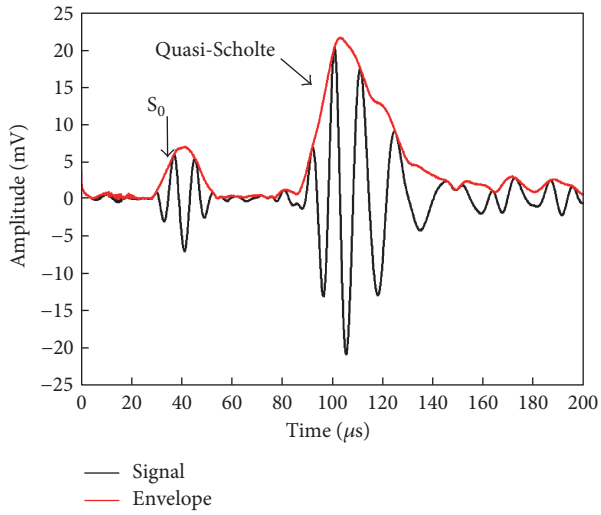

Figure 10: Experimental signal of guided waves in the plate with one side in water at 100 kHz.

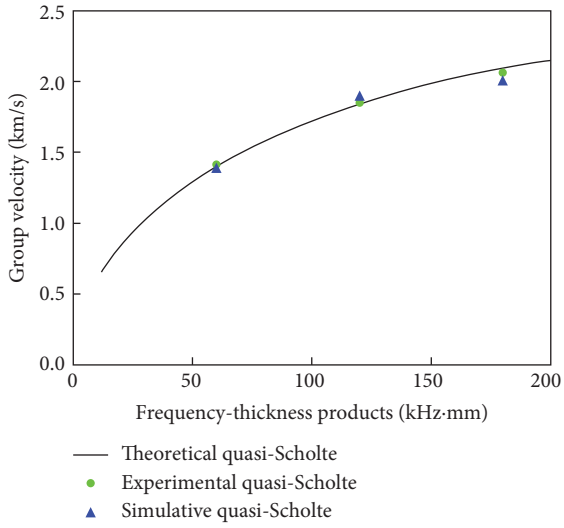

Figure 11: Comparison of quasi-Scholte mode's group velocities obtained from theory, simulation, and experiment.

As seen in (7), the water level d_W is linearly related to the time difference $\Delta t_{T\text{-}R}$.

4.2. Experimental Setup for Water Level Sensing. An experiment is performed using the configuration in Figure 12. The plate is a 1.2 mm thick steel with material properties given in Table 1. Two PZT transducers (with dimensions of $7 \times 7 \times 0.2$ mm) are bonded on the plate in a pitch-catch configuration with the distance of 100 mm. The excitation signal has 2.5-cycle tone bursts, generated by an arbitrary function generator (model: Tektronix AFG 3022). The amplitude of the excitation signal is 10 V, which is the maximum output of our function generator. With this amplitude, we can achieve the optimal signal-to-noise ratio within the capability of our current equipment. In this water level sensing test, the

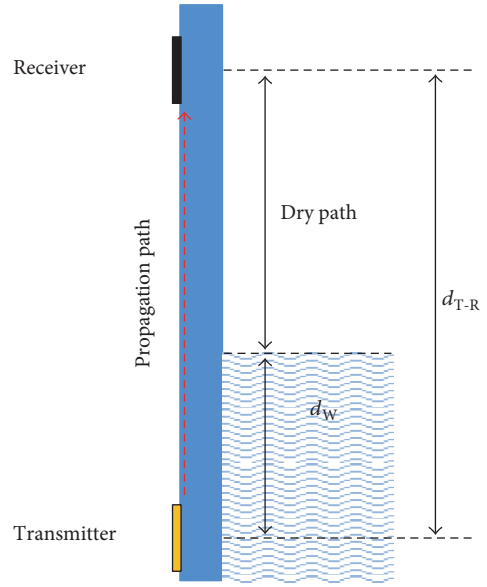

Figure 12: A pitch-catch configuration with two PZT transducers for water level sensing.

excitation frequency is selected at 130 kHz for the proof of concept. The guided waves excited by the actuator propagate along the plate. At the receiver, waves are measured by an oscilloscope (Tektronix TDS 2022B).

4.3. Data Analysis Using Pseudo Wigner-Vile Distribution (PWVD). Time-frequency analysis is a description of a signal in the time and frequency domain, indicating the energy distribution of the signal in the time-frequency space [22–27]. For signal analysis, this study employs PWVD. The measured experimental signal at the 50 mm water level is used as an example. The received waveform at the 50 mm water level is given in Figure 13(a). The traveling time of the second wave packet is contributions of both the A_0 and quasi-Scholte modes. Since the low-frequency A_0 and quasi-Scholte modes are highly dispersive, this dispersive effect may influence the measurement of travelling time of a wave packet. To precisely determine the travelling time at a certain frequency, time-frequency analysis is needed. Figure 13(b) plots a 2D time-frequency distribution of the PWVD. Figure 13(c) plots an extracted PWVD result at 130 kHz. Hence, the travelling time of the second wave package at 130 kHz can be determined.

4.4. Experimental Results. To investigate the relationship between the water level and the received signal, signals at the receiver are collected at a series of water levels from 0 mm to 100 mm with a step of 10 mm. Figure 14(a) plots four representative signals when the water levels are 0, 30, 60, and 100 mm. As shown in Figure 14(a), with the increase of water level, the wave packet gradually shifts to the right, which means the travelling time gradually increases. Using the PWVD method, the traveling time and time difference $\Delta t_{T\text{-}R}$ at 130 kHz are obtained. Figure 14(b) plots the derived time difference $\Delta t_{T\text{-}R}$ with respect to water level d_W. A linear fitting is applied to the experimental data. The fitting result is

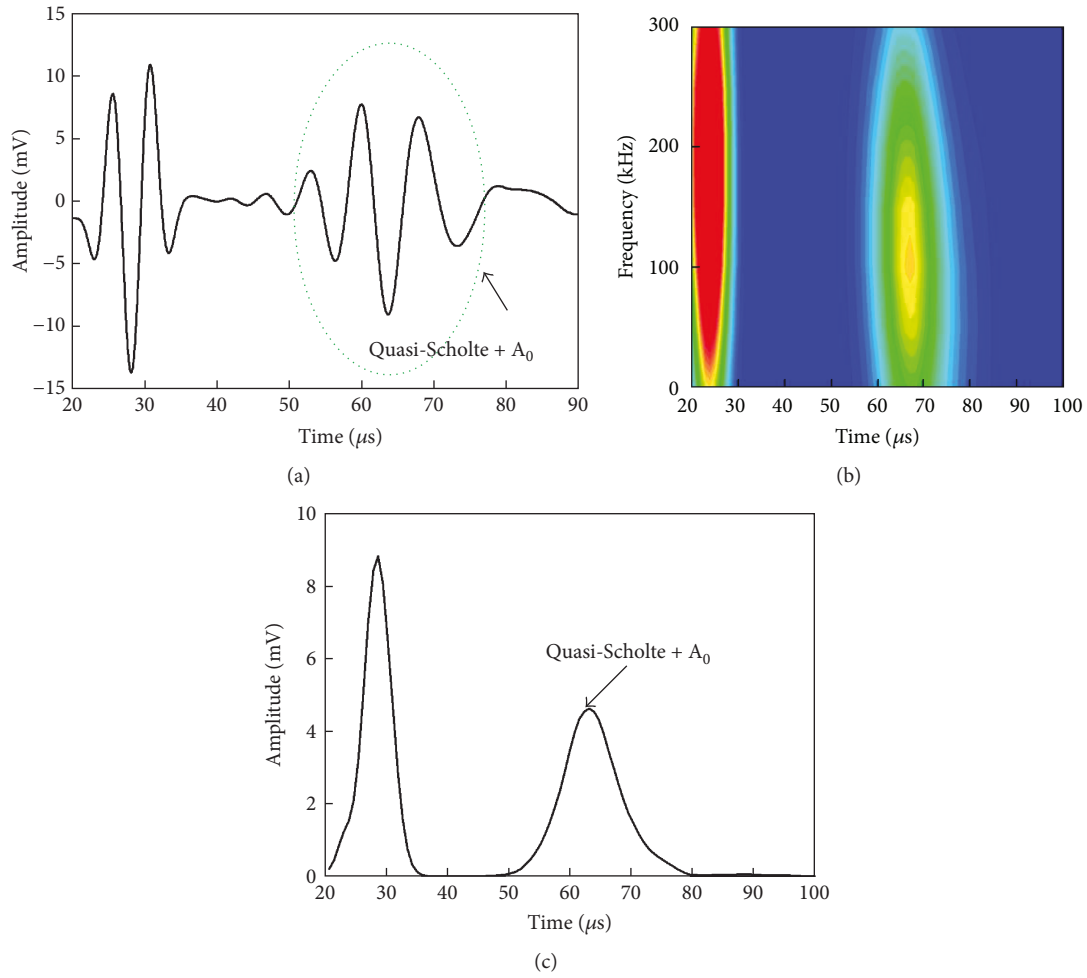

FIGURE 13: Analysis of a received signal using the PWVD: (a) received signal at the water level of 50 mm, (b) the PWVD result in time-frequency domain, and (c) the result of PWVD at 130 kHz.

$\Delta t_{\text{T-R}} = 0.034 d_{\text{W}}$ with the R^2 value of 0.998, which is close to 1. This means that the experimental results are in a linear relationship. The theoretical prediction derived from (7) is $\Delta t_{\text{T-R}} = 0.035 d_{\text{W}}$, which is also plotted in Figure 14(b). The coefficient of the linear fitting is very close to that of the theoretical prediction with an error of 2.9%. In addition, it can be seen that the experimental result agrees well with the theoretical prediction. The error for water level sensing is less than 3.7 mm. The precision of our method could be influenced by several factors including sensor installation errors, structural damage (corrosion, rust, and crack), environmental conditions, errors of wave speeds, and errors of the time differences. The measuring range depends on the distance between the actuator and the receiver. In the current setup, the distance is 100 mm, and thus the measuring range is 0~100 mm.

5. Conclusions

This paper presents a water level sensing method by using the A_0 and quasi-Scholte modes. The water level sensing method adopts a pitch-catch sensing configuration with a pair of PZT transducers bonded on a steel vessel. The travelling time of guided waves between the two transducers is influenced by the water level. Hence, by measuring the travelling time, the water level in the vessel can be found.

This study investigates the difference between guided waves in a free plate and a plate with one side. Through theoretical, numerical, and experimental studies, it is confirmed that the A_0 mode presents in a free plate and the quasi-Scholte mode presents in a plate with one side in water at low frequencies. Moreover, the A_0 mode can convert to the quasi-Scholte mode and vice versa. Lastly, the group velocity of the quasi-Scholte mode is smaller than that of the A_0 mode. Based on these findings, a water level sensing method is developed, which takes the advantage of the group velocity difference between the quasi-Scholte and A_0 modes.

The water level sensing method adopts a pair of PZT transducers in the pitch-catch configuration bonded on the out surface of the vessel. When the water level is between the two transducers, the entire travelling path can be divided into two portions, the dry path (with A_0 mode) and the water path (with quasi-Scholte mode). If the water level changes, the lengths of dry path and water path change; hence, the total travelling time changes. Based on this principle, the water level can be predicted by using

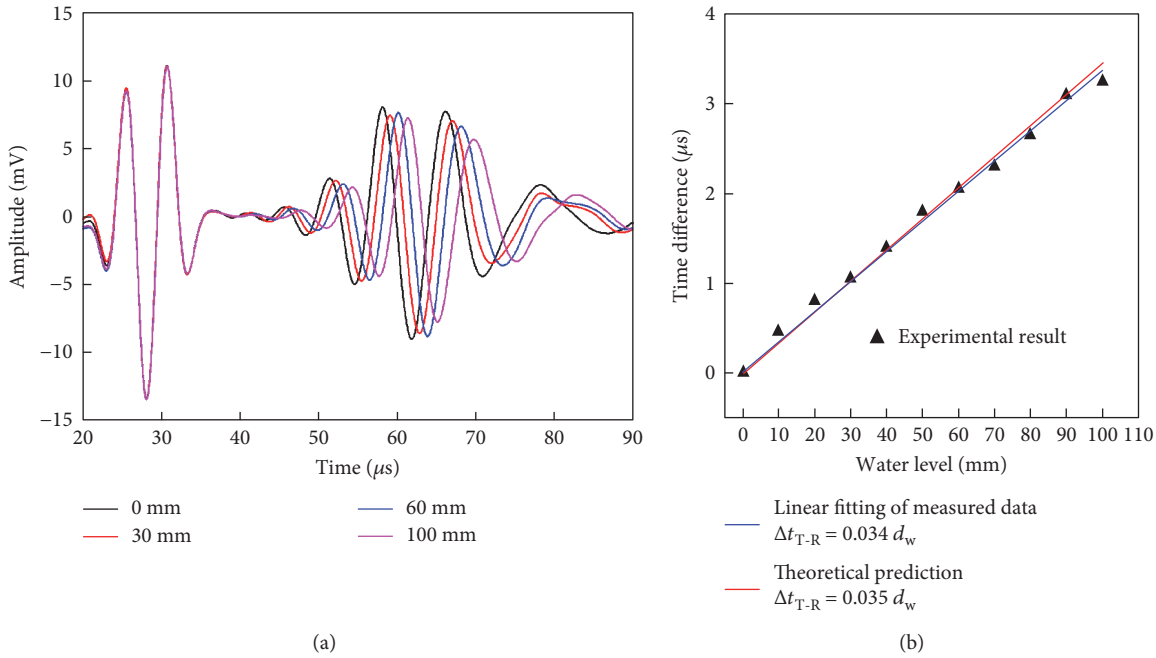

FIGURE 14: Experimental results. (a) Received waveforms at different water levels. (b) Water level sensing results. The linear fitting result shows that the water level d_W is in a linear relationship with the time difference $\Delta t_{T\text{-}R}$. In addition, experimental results agree well with the theoretical predictions.

the travelling time. For the proof of concept, we experimentally demonstrate water level sensing using guided waves. The experimental results show that wave travelling time linearly increases with the increase of water level and agree well with theoretical predictions.

For our method, the sensing resolution could be influenced by the wave speed, sampling rate of the data acquisition equipment, and the smallest time difference that can be determined. The sensitivity could be influenced by the wave speed difference between the A_0 mode and the quasi-Scholte mode. In the future, we will perform detailed parametric studies with both theoretical analysis and experiments, in order to characterize the sensing resolution and sensitivity, as well as identify the optimum frequency that can provide the best sensing resolution and sensitivity. For real-world applications, there are still some challenges. Our method could be influenced by structural damage (corrosion, rust, and crack), temperature fluctuation, and sensor degradation under harsh environmental conditions. In the future, we aim to develop a more robust system with these challenges considered for practical applications in power plants.

Conflicts of Interest

The authors declare that there is no conflict of interest regarding the publication of this paper.

Acknowledgments

The authors would like to acknowledge and thank (1) National Natural Science Foundation of China (51134016, 11074073) and (2) the Fundamental Research Funds for the Central Universities (2016XS25).

References

[1] J. L. Rose, *Ultrasonic Waves in Solid Media*, Cambridge University Press, Cambridge, 1999.

[2] V. Giurgiutiu, *Structural Health Monitoring with Piezoelectric Wafer Active Sensors*, Academic Press, Boston, MA, USA, 2008.

[3] D. C. Worlton, *Ultrasonic Testing with Lamb Waves*, General Electric Co., Hanford Atomic Products Operation, Richland, Washington, 1956.

[4] D. N. Alleyne and P. Cawley, "The interaction of lamb waves with defects," *IEEE Transactions on Ultrasonics, Ferroelectrics, and Frequency Control*, vol. 39, no. 3, pp. 381–397, 1992.

[5] D. C. Worlton, "Experimental confirmation of lamb waves at megacycle frequencies," *Journal of Applied Physics*, vol. 32, no. 6, pp. 967–971, 1961.

[6] J. Bingham, M. Hinders, and A. Friedman, "Lamb wave detection of limpet mines on ship hulls," *Ultrasonics*, vol. 49, no. 8, pp. 706–722, 2009.

[7] W. B. Na and T. Kundu, "Underwater pipeline inspection using guided waves," *Transactions-American Society of Mechanical Engineers Journal of Pressure Vessel Technology*, vol. 124, no. 2, pp. 196–200, 2002.

[8] J. Chen, Z. Su, and L. Cheng, "Identification of corrosion damage in submerged structures using fundamental anti-symmetric lamb waves," *Smart Materials and Structures*, vol. 19, no. 1, article 015004, 2009.

[9] J. P. Koduru and J. L. Rose, "Mode controlled guided wave tomography using annular array transducers for SHM of water loaded plate like structures," *Smart Materials and Structures*, vol. 22, no. 12, article 125021, 2013.

[10] E. Pistone, K. Li, and P. Rizzo, "Noncontact monitoring of immersed plates by means of laser-induced ultrasounds," *Structural Health Monitoring*, vol. 12, no. 5-6, pp. 549–565, 2013.

[11] C. L. Yapura and V. K. Kinra, "Guided waves in a fluid-solid bilayer," *Wave Motion*, vol. 21, no. 1, pp. 35–46, 1995.

[12] C. Baron and S. Naili, "Propagation of elastic waves in a fluid-loaded anisotropic functionally graded waveguide: application to ultrasound characterization," *The Journal of the Acoustical Society of America*, vol. 127, no. 3, pp. 1307–1317, 2010.

[13] L. Yu and Z. Tian, "Case study of guided wave propagation in a one-side water-immersed steel plate," *Case Studies in Nondestructive Testing and Evaluation*, vol. 3, pp. 1–8, 2015.

[14] S. Banerjee and T. Kundu, "Ultrasonic field modeling in plates immersed in fluid," *International Journal of Solids and Structures*, vol. 44, no. 18-19, pp. 6013–6029, 2007.

[15] M. Cui, F. Tian, Y. Li, and J. Wang, "Research on uncertainty evaluation of the compensated differential pressure level measurement," *Chinese Journal of Mechanical Engineering*, vol. 37, no. 7, pp. 1524–1531, 2016.

[16] V. E. Sakharov, S. A. Kuznetsov, B. D. Zaitsev, I. E. Kuznetsova, and S. G. Joshi, "Liquid level sensor using ultrasonic lamb waves," *Ultrasonics*, vol. 41, no. 4, pp. 319–322, 2003.

[17] H. H. Hao and J. Q. Xiong, "A method of liquid level measurement based on ultrasonic echo characteristics," in *2010 International Conference on Computer Application and System Modeling (ICCASM 2010)*, pp. V11–682–V11–684, Taiyuan, China, October 2010.

[18] Z. Qingqing, "Study on measurement of guided wave radar level gauge technology," *Electronic Instrumentation Customers*, vol. 24, no. 3, pp. 23–27, 2017.

[19] H. Lamb, "On waves in an elastic plate," *Proceedings of the Royal Society of London A: Mathematical, Physical and Engineering Sciences*, vol. 93, no. 648, pp. 114–128, 1917.

[20] F. B. Cegla, P. Cawley, and M. J. S. Lowe, "Material property measurement using the quasi-Scholte mode—a waveguide sensor," *The Journal of the Acoustical Society of America*, vol. 117, no. 3, pp. 1098–1107, 2005.

[21] F. B. Cegla, P. Cawley, and M. J. S. Lowe, "Fluid bulk velocity and attenuation measurements in non-Newtonian liquids using a dipstick sensor," *Measurement Science and Technology*, vol. 17, no. 2, p. 264, 2005.

[22] L. Cohen, "Time-frequency distributions: a review," *Proceedings of the IEEE*, vol. 77, no. 7, pp. 941–981, 1989.

[23] W. J. Williams, "Cross Hilbert time-frequency distributions," in *Proceedings SPIE 3461, Advanced Signal Processing Algorithms, Architectures, and Implementations VIII*, pp. 120–129, San Diego, CA, USA, October 1998.

[24] L. B. White and B. Boashash, "Cross spectral analysis of nonstationary processes," *IEEE Transactions on Information Theory*, vol. 36, no. 4, pp. 830–835, 1990.

[25] B. Boashash and P. O'shea, "Use of the cross Wigner-Ville distribution for estimation of instantaneous frequency," *IEEE Transactions on Signal Processing*, vol. 41, no. 3, pp. 1439–1445, 1993.

[26] L. Yu, Y. Shin, J. Wang, and Y. Shen, "An ultrasonic guided wave sensor for gas accumulation detection in nuclear emergency core cooling systems," *8th International Workshop on Structural Health Monitoring*, DEStech Publications, Inc., Lancaster, PA, USA, 2011.

[27] L. Yu, B. Lin, Y. J. Shin, J. Wang, and Z. Tian, "Ultrasonic gas accumulation detection and evaluation in nuclear cooling pipes," in *Proceedings SPIE 8345, Sensors and Smart Structures Technologies for Civil, Mechanical, and Aerospace Systems 2012*, p. 83454U, San Diego, CA, USA, April 2012.

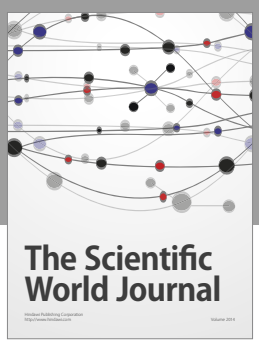

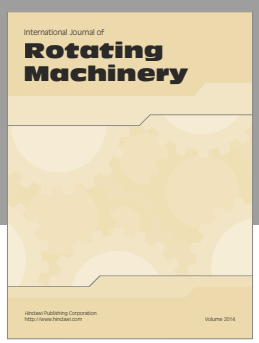

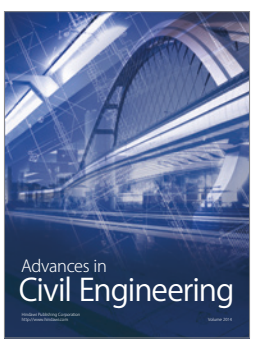

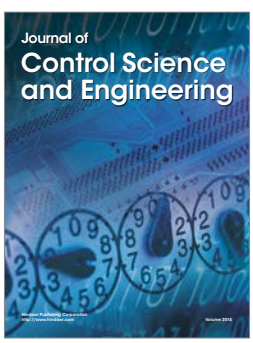

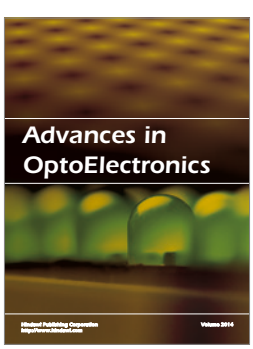

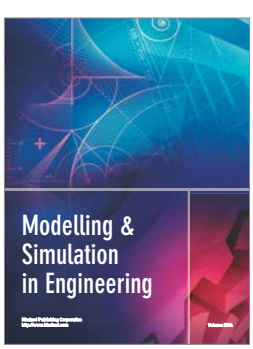

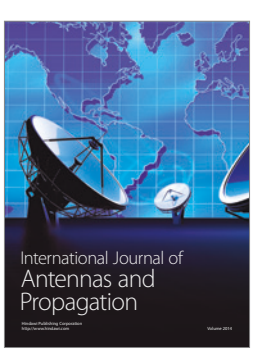

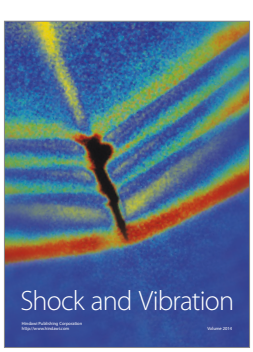

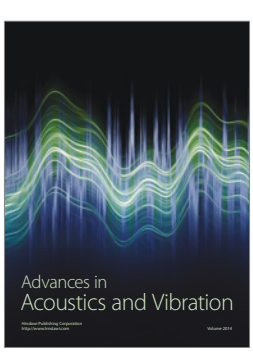

Hindawi

Submit your manuscripts at
https://www.hindawi.com